Supplementary Information to "Predicting Mechanical Properties of Non-Equimolar High-Entropy Carbides using Machine Learning"

S1 – The crystal structures for high-throughput density functional calculations of elastic properties for 495 carbides and 123 high-entropy carbides

The crystal structure (left) used for the calculation of the elastic properties of 495 carbides is a single-phase salt rock structure with 8 atoms, and the crystal structure (right) used for the calculation of the elastic properties of 123 high-entropy carbides is a 2x1x1 single-phase salt rock structure containing 16 atoms. For all calculation structures, transition metal atoms Ta, Zr, Hf, V, Nb, Ti, Mo, W, Cr occupy the cation sites and carbon atoms occupy the anion sites.

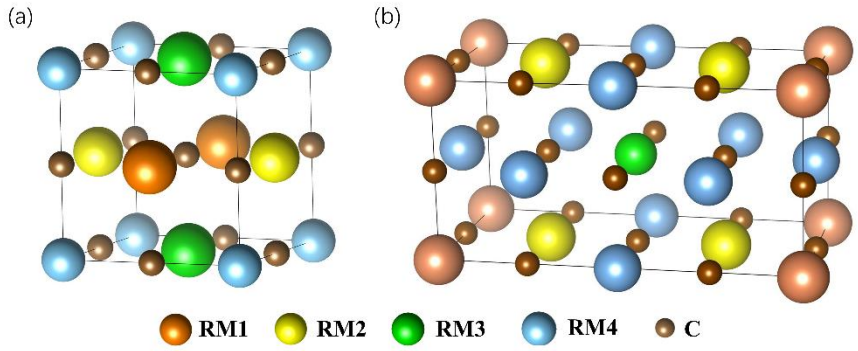

Fig S1 Calculation structure for carbides and high entropy carbides

S2 – The elastic properties of monocarbides

The elastic modulus of monocarbides is employed to calculate the ROM values of the elastic properties for 495 carbide systems.

Table S1 . The elastic properties of binary carbides

Binary Carbide	Young's modulus (GPa)	bulk modulus (GPa)	shear modulus (GPa)
ZrC	393.59	222.63	163.27
NbC	436.19	301.31	173.27
HfC	452.36	254.57	187.88
TaC	421.97	338.65	163.26
TiC	438.54	266.74	178.85
CrC	427.71	338.28	165.87
VC	556.30	318.72	230.05
MoC	436.19	301.31	173.27
WC	424.41	381.01	161.45

S3 – The machine learning predicted elastic properties of 495 carbides with five kinds of composition-based feature vector descriptors

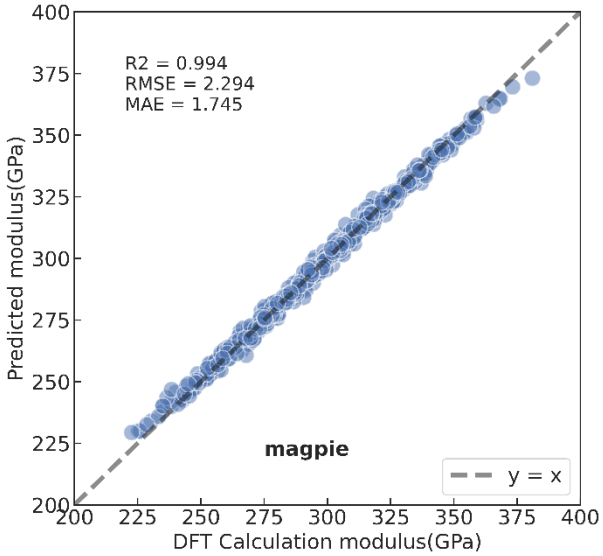

Fig S8 Machine learning prediction results with magpie descriptors

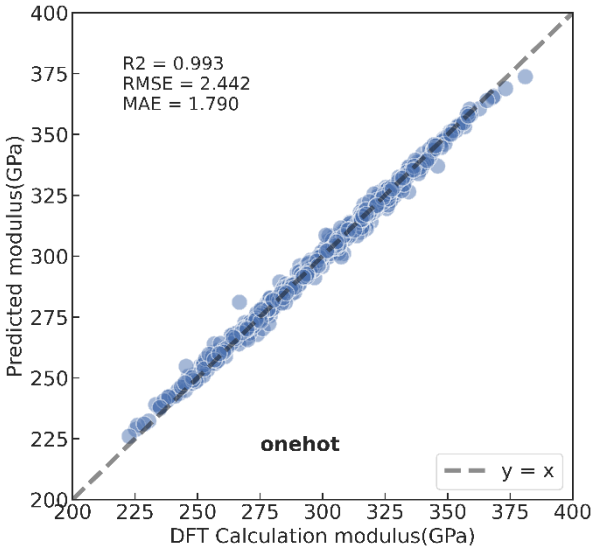

Fig S9 Machine learning prediction results with onehot descriptors

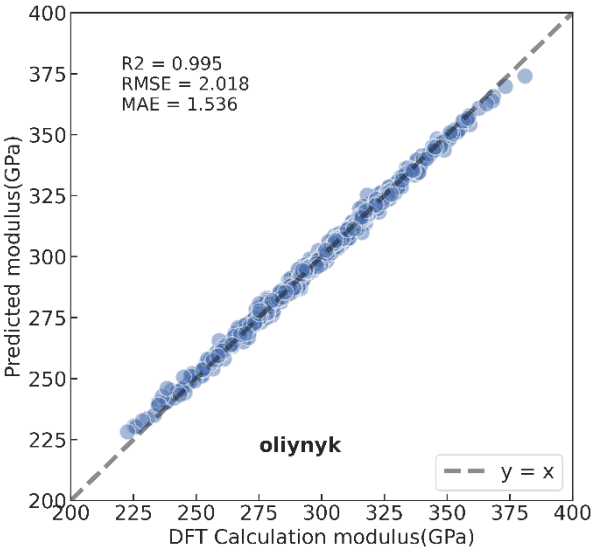

Fig S10 Machine learning prediction results with oliynyk descriptors

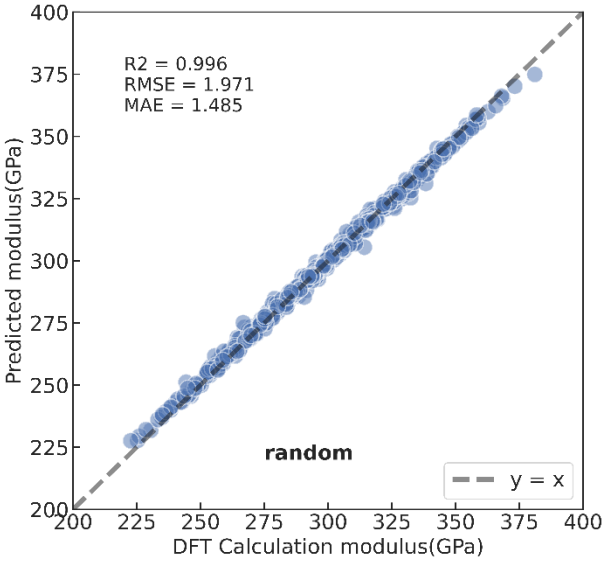

Fig S11 Machine learning prediction results with random descriptors

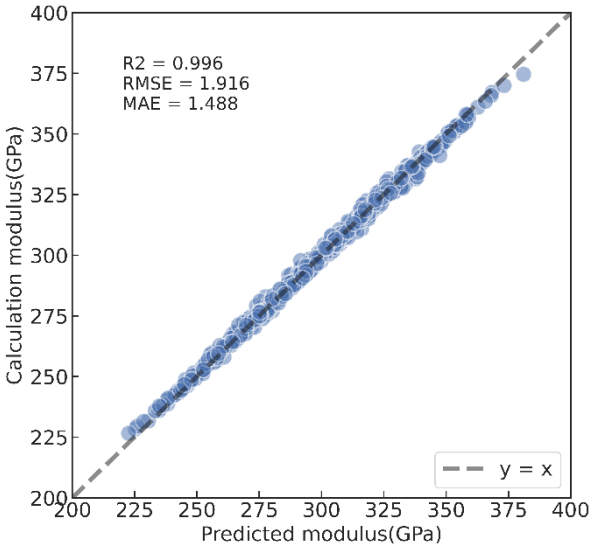

Fig S12 Machine learning prediction results with mat2vec descriptors

S4 –Results of Crabnet model predicting elastic properties

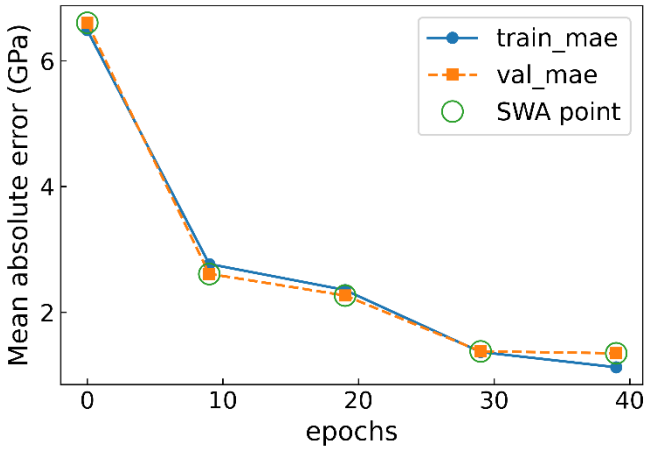

Fig S13 The changes in predicted Young's modulus over the course of the optimization process against the mean absolute error

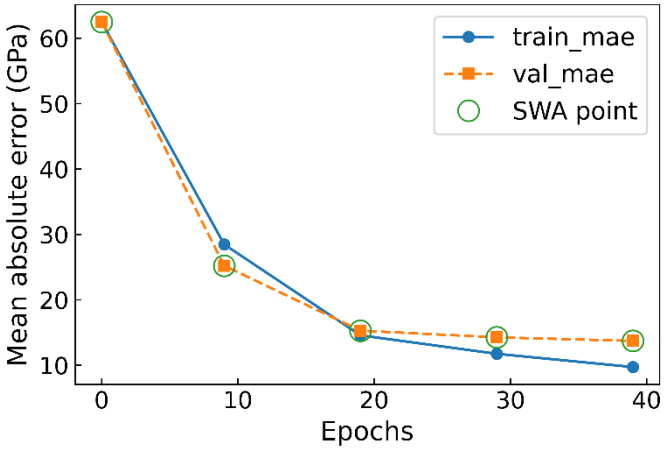

Fig S14 The changes in predicted hardness over the course of the optimization process against the mean absolute error